University of Central Florida

STARS

Electronic Theses and Dissertations

2019

ATP Induced Molecular Disassembly of Cytolethal Distending Toxin's B/C Heterodimer

George Huhn
University of Central Florida

ATP-INDUCED DISASSEMBLY OF THE CDTB/CDTC HETERODIMER OF
CYTOLETHAL DISTENDING TOXIN

by

GEORGE ROBB HUHN III

B.S. University of Central Florida, 2016
A.A. Valencia College, 2010

A thesis submitted in partial fulfillment of the requirements
for the degree of Master of Science in Biotechnology
in the Burnett School of Biomedical Sciences
in the College of Medicine
at the University of Central Florida
Orlando, Florida

Summer Term
2019

Major Professor: Ken Teter

ABSTRACT

Cytolethal distending toxin (CDT) is a virulence factor produced by many Gram-negative bacteria, including *Haemophilus ducreyi.* This fastidious pathogen is the causative agent of genital cancroid. CDT is a heterotrimeric toxin with an AB_2 structure consisting of a cell-binding "B" domain (CdtA + CdtC) and a catalytic "A" domain (CdtB) that has DNase activity. This toxin assembles in the bacterial periplasm that lacks ATP and is secreted into the extracellular environment. After cell binding, CDT is internalized by endocytosis and travels through the endosomes and Golgi before arriving in the endoplasmic reticulum (ER). CdtA is lost from the holotoxin before reaching the Golgi, and CdtB separates from CdtC in the ER. CdtB is then transported into the nucleus, inducing cell cycle arrest and apoptosis. Using disassembly of the AB_5 pertussis toxin as a model, we explore that ATP, which is present in the ER lumen but not in the endosomes or Golgi, will cause dissociation of the CdtB/CdtC heterodimer. We have cloned and purified the three individual subunits of the *H. ducreyi* CDT. When combined, the subunits form a lethal holotoxin. Examining the individual toxin subunits, only CdtB binds with ATP but does not function as an ATPase. CdtB's binding to ATP also does not cause global changes to its secondary structure. After isolating the CdtB/CdtC heterodimer, we have shown the addition of ATP causes CdtC to dissociate from CdtB. The work presented in this Thesis provides a molecular basis for why the CdtB/CdtC heterodimer disassembles after reaching the ER and confirms the novel two-stage disassembly mechanism for CDT, a first in the AB toxin field.

I dedicate this to my parents, Cindy Huhn and George Robb Huhn II for not giving up on me during my extended undergraduate career.

ACKNOWLEDGMENTS

TABLE OF CONTENTS

LIST OF FIGURES

LIST OF TABLES

CHAPTER 1: INTRODUCTION AND BACKGROUND

Cytolethal distending toxin (CDT) is a virulence factor produced by many Gram-negative pathogens including *Haemophilus ducreyi*, *Escherichia coli*, *Campylobacter jejuni*, and *Aggregatibacter actinomycetemcomitans* [1]. This thesis focuses on the CDT produced by *H. ducreyi*, a fastidious Gram-negative coccobacillus linked to a sexual transmitted infection (STI) prevalent in Africa known as genital chancroid [2-4]. CDT contributes to the infectious process by inducing apoptosis in lymphocytes, thus allowing bacterial persistence at the site of infection by inhibiting an adaptive immune response [5, 6].

Structure

CDT is part of the AB toxin family, which includes a large group of bacterial toxins that share a common structural organization comprised of a catalytic A subunit and a cell binding B subunit. CDT is a heterotrimeric AB_2 genotoxin with one catalytic protein (CdtB) and two cell-binding proteins (CdtA and CdtC) (Fig. 1). It is encoded by the *cdt* operon contained in the bacterial genome, with *cdtB* located between *cdtA* and *cdtC* [7]. The genes in an operon are labeled alphabetically in the order they are transcribed, explaining why the catalytic A protein is identified as the CdtB subunit. After translation, the holotoxin spontaneously assembles in the neutral pH environment of the bacterial periplasm and is secreted into the extracellular space. Unlike most other AB toxins, CDT does not have disulfide linkages to maintain holotoxin structure [7]. Noncovalent protein-protein interactions are sufficient to assemble and maintain a stable CDT holotoxin [7].
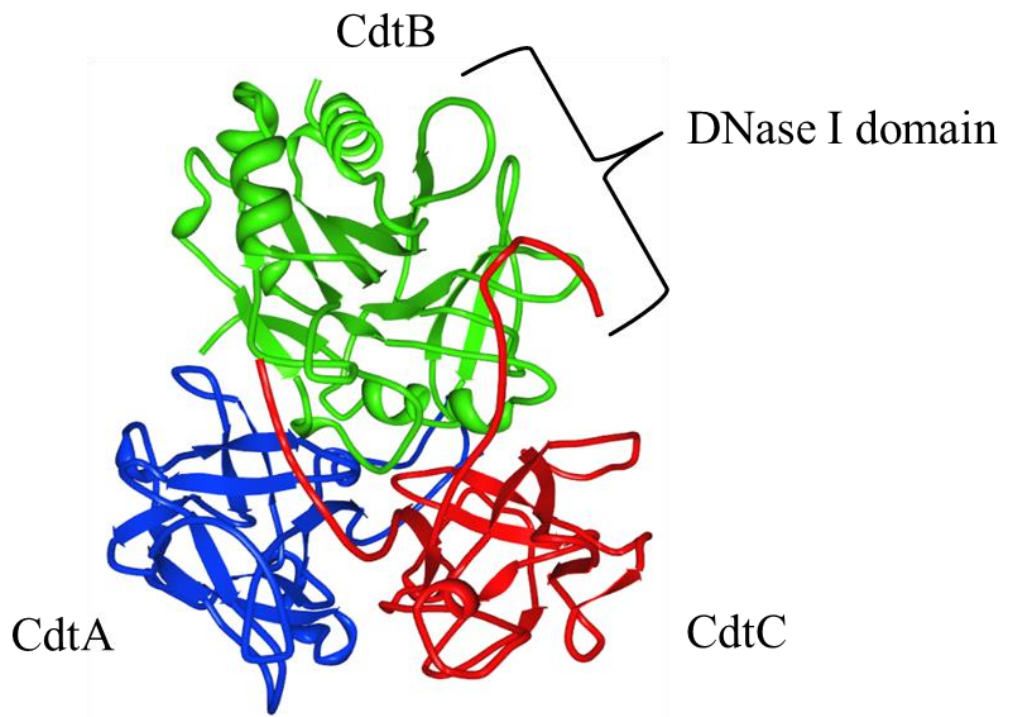
Figure 1: Ribbon diagram of CDT holotoxin.

CDT is a heterotrimeric AB_2 toxin. CdtA (blue) and CdtC (red) make up the cell binding "B" domain. CdtB (green) is the catalytic "A" domain. The N-terminal region of CdtC is seen blocking the active site of the DNase I domain in CdtB, requiring toxin disassembly to activate the latent DNase activity of CdtB. PDB 1SR4 [7, 8]

Function

CdtA and CdtC make up the cell binding "B" domain that binds to lipid rafts, specific regions with high cholesterol in the plasma membrane [9, 10]. Both subunits also contain lectin motifs that are similar to the cell-binding subunit of ricin, another AB toxin [11]. Lectin motifs recognize specific glycan modifications present on proteins and lipids, but the exact configuration of sugar residues on CDT surface receptors has not yet been identified for HdCDT [12]. Lipid rafts are required for intoxication while the lectin binding interactions only play an accessory role [9, 10, 12].

CdtB is the catalytic A subunit that contains structural similarities to the DNase I endonuclease family [7]. Like DNase I, CdtB can cause double-stranded DNA breaks [13, 14]. This triggers a DNA repair response mediated by ataxia-telangiectasia mutated (ATM), a kinase that phosphorylates the H2AX histone. This modification recruits the MRN complex to repair DNA either by homologous recombination or non-homologous end joining repair [10, 15]. During this process, the cell cycle will be arrested during G1 or G2 phase [16]. Cellular expansion is still active during this arrest, leading to a distended phenotype. If DNA repair is successful, the cell will resume through the cell cycle. Failure will induce apoptosis.

Trafficking

In order for CdtB to reach the DNA, it must travel from the extracellular space to the nucleus [6, 17]. This pathway involves several steps, including (i) CDT holotoxin binding to the host plasma membrane binding; (ii) internalization in a clathrin- and dynamin-dependent manner; (iii) vesicle transport passing through the early and late endosomes before reaching the Golgi apparatus; and (iv) retrograde transport from the Golgi apparatus to the endoplasmic reticulum (ER). After

reaching the ER, only CdtB is transported into the nucleus where it causes double-stranded breaks in the host DNA [10, 13, 18-21].

Two-Stage Disassembly

Although all three Cdt subunits are required for cellular intoxication, CdtC blocks CdtB active site, so disassembly is required to cause DNA damage after reaching the nucleus [18, 22, 23]. Confocal microscopy did not detect an intracellular pool of CdtA, which suggested CdtA is left on the cell surface while the CdtB/CdtC heterodimer is internalized [24]. However, this negative result does not eliminate the possibility of CdtA internalization and/or recycling. For example, CdtA could dissociate from CdtB/CdtC in the endosomes after holotoxin internalization and then return to the surface. Only CdtB and CdtC arrive at the Golgi apparatus after passing through the endosomes, as demonstrated by the sulfation of recombinant CdtB and CdtC but not CdtA [10, 25, 26]. Sulfation is a protein modification specific to the Golgi apparatus, so the lack of CdtA sulfation indicates that CdtA disassociated from the CdtB/CdtC heterodimer before their arrival to the Golgi [25, 26]. Whether CdtA dissociation from CdtB/CdtC occurs at the cell surface or in the endosomes, there is a consensus that CdtA is lost early in the transport pathway. This is the first stage of CDT disassembly. CdtB and CdtC are further transported to the ER demonstrated by confocal microscopy [24]. However, only CdtB delivery to the ER was confirmed by N-glycosylation, the attachment of glycans to asparagine amino acids that occurs in the ER. N-glycosylation was not tested with CdtC. [10, 27]. Since CdtB alone is transported to the nucleus, the intracellular transport of CDT involves a novel two-stage disassembly process as summarized in Figure 2.
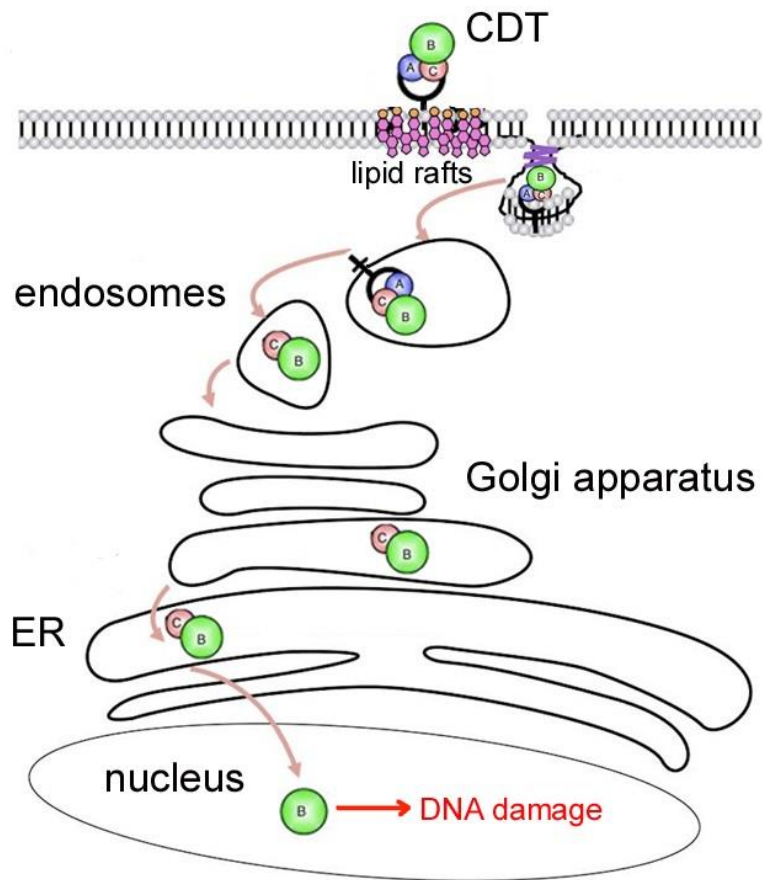
Figure 2: Intracellular transport and disassembly of CDT.

CDT undergoes retrograde transport passing through the endosomes and Golgi apparatus before arriving in the ER. CdtA dissociates from the CdtB/CdtC heterodimer before reaching the Golgi apparatus [25]. Only CdtB moves from the ER lumen into the nucleus. Adapted from [28].

CHAPTER 2: THESIS AIM AND RATIONALE

Thesis aim: Elucidate the molecular mechanism for CdtB/CdtC disassembly.

There are many CDT studies detailing its possible binding receptors, intracellular trafficking route, and cellular response mechanisms after intoxication. Yet the molecular mechanism by which CDT disassembles before ER translocation has not been addressed. After the crystal structure of HdCDT was solved in 2004, computer modeling showed that the N-terminal tail of CdtC is blocking the DNA binding site of CdtB. Thus, CdtB must separate from CdtC for DNase activity [7, 29]. The goal of this thesis is to detail the mechanism of how CdtB and CdtC dissociate while in the heterodimer conformation during intracellular transport.

Most AB toxins contain a disulfide bond that is necessary to maintain their structure and requires chaperone intervention for disassembly [30-32]. Pertussis toxin (PT), similar to CDT, is an ER-translocating AB toxin held together by noncovalent protein-protein interactions rather than a disulfide bond (Fig. 3) [33]. After transport into the ER, the catalytic S1 subunit of PT (PTS1) is released from its B pentamer (PTB) in an ATP-induced, chaperone-independent manner [34-36]. Disassembly results from ATP entering into the pore of the ring-like PTB pentamer, causing a conformational change that weakens the association between PTS1 and the PTB pentamer [35]. Using the disassembly of PT as a model, we hypothesize that ATP will induce the disassembly of the CdtB/CdtC heterodimer. ATP is not present in the bacterial periplasm, endosomes, or Golgi apparatus, but it is present in the ER [26, 37, 38]. ATP could thus act as a molecular sensor to activate CdtB/CdtC disassembly at the CdtB translocation site [37].

Previously, it has been shown by surface plasmon resonance (SPR) [39, 40] that CdtC will dissociate from the CdtB in the presence of ATP (Fig. 4). After CdtB was appended to the SPR slide, CdtC was injected into the profusion buffer and formed a stable complex with CdtB. Disassembly did not occur after a drop in pH, a characteristic in the endosomes [38]. Instead, disassembly occurred after the addition of ATP. The loss of CdtC and retention of CdtB was verified by the addition of subunit-specific polyclonal antibodies (Fig. 4). The CdtB/CdtC heterodimer will not encounter ATP until it reaches the ER. Thus, after delivering CdtB to the ER, CdtC will be released after which CdtB is then transported into the nucleus. Further characterization of this mechanism is presented here; this work provides a molecular basis for a key, but poorly understood event during CDT intoxication.
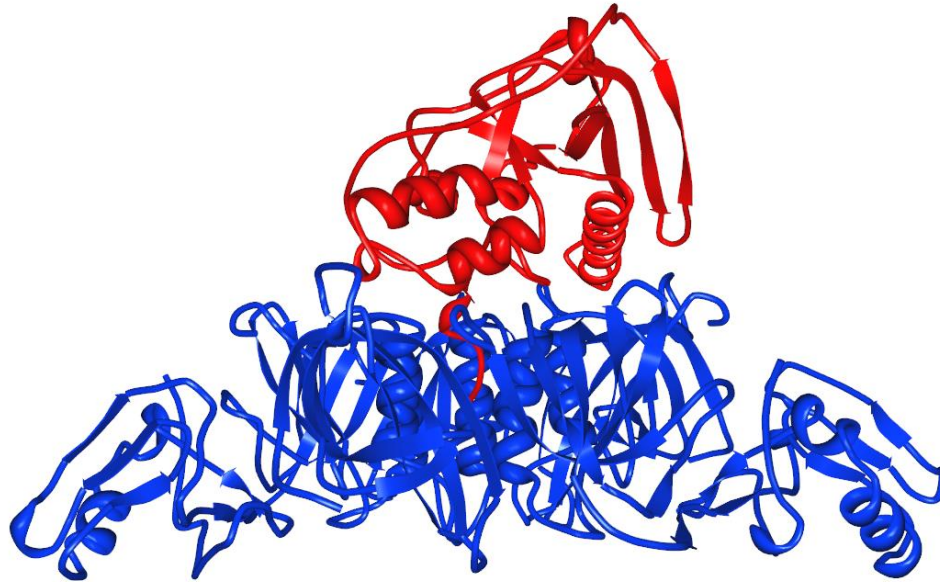
Figure 3: The ribbon diagram of pertussis toxin.

Pertussis toxin is an AB_5 toxin comprised of PTB and PTS1. The pentameric cell-binding B domain (blue) is made up of five proteins: S2, S3, S4 (two copies), and S5. PTS1 is the A catalytic domain (red). PDB 1PRT [33]
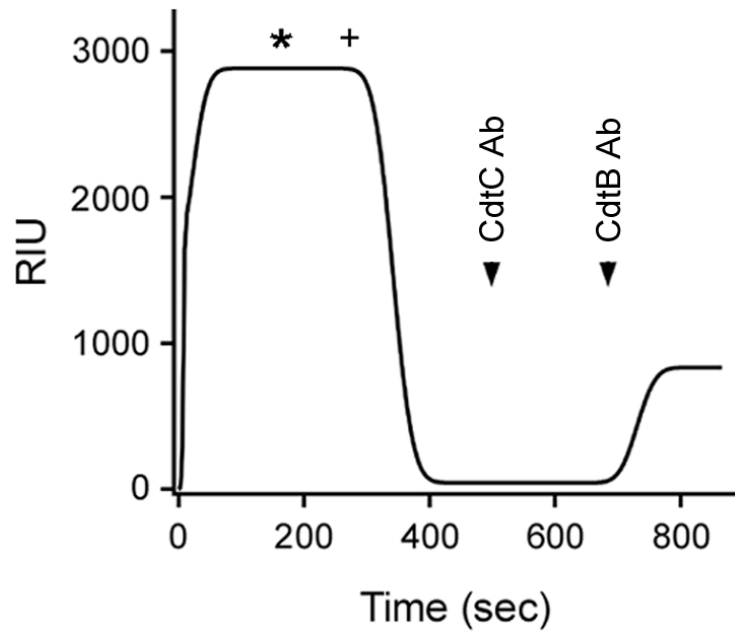
Figure 4: ATP disassembly of the CdtB/CdtC heterodimer detailed by SPR.

At 0 sec, CdtC was perfused over an SPR slide previously bound with CdtB. The buffer was changed to pH 5.2 at 180 sec (asterisk). At 350 sec, the pH was raised to 7.4 and 200 µM ATP was added to the buffer (plus sign). Anti-CdtC, then anti-CdtB antibodies were added at the indicated times. CdtC dissociated from CdtB with the addition of ATP, while CdtB remained bound to the SPR slide. This experiment was performed by Dr. Mike Taylor and John Clore.

Significance and implication

The CDT produced by *H. ducreyi* has been shown to induce apoptosis in B-lymphocytes, T-lymphocytes, and immature dendritic cells - all key cells in the adaptive immune response [5, 41, 42]. Currently, there are no studies focused on CDT's disassembly. Host-toxin interactions involving CDT have mainly focused on identifying the cell-binding event, intracellular transport route, or cellular response mechanisms. CDT is the first AB toxin that has two stages of disassembly, but the mechanism and rationale for this two-stage event are unknown. Understanding this disassembly mechanism can provide additional information that could establish alternative treatment methods for CDT-producing bacterial infections. Preventing disassembly of CDT may prevent CdtB from generating DNA damage. This, in turn, could inhibit the effect seen in adaptive immune cells that restricts the humoral response and could thereby provide an alternative to antibiotic treatments.

CHAPTER 3: MATERIALS AND METHODS

CDT toxin subunits

- Dr. Tersea Frisan (Karolinska Institutet; Stockholm, Sweden) generously gifted *cdtA*, *cdtB*, and *cdtC* coding sequences that were inserted into the bacterial expression vector pGEX3T3.

- Insertion of the *cdt* coding sequences into the pET-28(a) bacterial expression vector was previously done by Dr. Lucia Cilenti.

Additional cloning of Cdt subunits

Glycerol stocks of *Escherichia coli* strain DH5α carrying pET-28(a) plasmids encoding for CdtA, CdtB, or CdtC were streaked onto sterile lysogeny broth (LB) agar plates containing 50 µg/mL of kanamycin and 0.02% glucose [43]. Individual colonies were selected and inoculated in 5 mL of sterile LB containing 50 µg/mL kanamycin and 0.02% glucose. Plasmid DNA was harvested using Macherey-Nagel's (Bethlehem, PA) Nucleospin Plasmid kit. Using 'Round-the-horn [44] site-directed mutagenesis, plasmids were amplified using the Thermo Scientific™ (Waltham, MA) Phusion Site-Directed Mutagenesis Kit. The primers used are detailed in Table 1. After ligation, DNA was transformed into DH5α cells using a one-step transformation method [45]. After recovery for 1 h at 37°C with shaking in 1 mL of LB, the cells were pelleted at 5000 × g for 5 min, resuspended in 100 µL of LB, and plated onto LB agar plates containing 50 µg/mL of kanamycin and 0.02% glucose. Multiple colonies were selected and grown individually overnight in 6 mL of LB containing 50 µg/mL of kanamycin and 0.02% glucose. Glycerol stocks of DH5α cells were generated by combining 900 µL of the individual cultures with 900 µL of PBS (pH 7.4) containing 50% glycerol and stored at -80°C. Plasmid DNA was harvested from the remaining inoculum and

sent for sequencing. After verification of the deletion, the plasmid DNA was transformed into *E. coli* strain BL21(DE3)pLysS using the transformation method above and plated on LB agar plates containing only 50 µg/mL of kanamycin. Glycerol stocks for the individual subunits were generated as described above and kept at -80°C. The addition of glucose with DH5α cells was to increase bacterial growth, in turn increasing potential DNA recovery yield of the low-copy pET-28(a) plasmid. For BL21(DE3)pLysS growth, glucose was absent in order to prevent bacterial stress incurred by the diauxic transition to LB media metabolism that would inhibit protein production.

Table 1: Primers used for subcloning *cdt* sequences

Primer Name	Primer sequence 5´ – 3´
CdtA forward	ATGCATCATCATCATCATCACTGTTCATCAAATCAACGAATGAATGAC
CdtB forward	ATGCATCATCATCATCATCACAACTTGAGTGACTTCAAAGTAGCAAC
CdtC forward	ATGCATCATCATCATCATCACAGTCATGCAGAATCAAATCCTGATCCG
pET-28(a) reverse	GGTATATCTCCTTCTTAAAGTTAAACAAAATTATTTCTAGAGGGGAATTGTTATCCGC

List of DNA primers used for 'Round-the-horn site-directed mutagenesis of *cdt* coding sequences. All sequences were contained in the pET-28(a) bacterial expression vector with a N-terminal hexahistidine sequence. Each plasmid contained a linker region between the N-terminal hexahistidine tag and subunit coding sequence. The forward primers were used to amplify the subunit coding sequence with the incorporation of a hexahistidine tag, while the reverse was used to amplify the vector. The pET-28(a) reverse primer served as the reverse primer for each reaction.

Protein purification

E. coli strain BL21(DE3)pLysS carrying a pET-28(a) plasmid containing the correct subunit sequence was streaked onto LB agar plates containing 50 µg/mL of kanamycin from glycerol stocks. An individual colony was incubated overnight in 5 mL of LB containing 50 µg/mL kanamycin, then expanded into 1 L of LB at the same antibiotic concentration. After reaching an O.D.$_{600}$ between 0.4 to 0.6, the culture was induced with 1 mL of 1 M IPTG and incubated for an additional 4 to 6 h. Induced cultures were then pelleted by centrifugation, spinning at $6,000 \times g$ for 20 min. Pellets were resuspended in 20 mM Tris (pH 7.5) with 25 mM NaCl and pelleted again to remove any remaining LB media. Pellets were stored at -80°C until protein extraction.

Bacterial cells were lysed using B-PER II (ThermoScientific; Waltham, MA) containing 100 µg/mL lysozyme (reconstituted in 1 mL of 20 mM Tris pH 7.4 with 150 mM NaCl), shaking at 150 rpm for 20 min at 37°C, followed by centrifugation at $12,000 \times g$ for 30 min. Since neither of the subunits are solubly expressed in viable quantities, the supernatant was discarded, and the insoluble pellet was solubilized with rocking at 4°C for 2 h in 50 mM Tris (pH 8.0) containing 300 mM NaCl and 8 M urea. The now-soluble protein solution was added to a 2 mL bed volume TALON Cobalt Metal Affinity Resin (Takara Bio; Mountain View, CA) for 2 h, allowing for efficient His-tag binding. The slurry was spun down at $500 \times g$ for 5 min. The supernatant was collected and labeled as "Did Not Bind". The TALON beads were then resuspended in 15 mL of 50 mM Tris (pH 7.0) with 600 mM NaCl and 8 M urea, gently rocked for 15 min and transferred into a gravity column. The flow through was collected and labeled as "Wash 1". The TALON beads were further washed with three column volumes of 50 mM Tris (pH 7.0) with 300 mM

NaCl, 8 M urea, and 10 mM imidazole. The collected flow-through was labeled as "Wash 2".

Proteins were then eluted in an increasing imidazole gradient, starting at 20 mM and finishing at

300 mM, in 20 mM Tris (pH 7.0). Fractions were visualized via 15% Tris-glycine SDS-PAGE gel

and Coomassie stain. Fractions selected based on purity were then dialyzed against 20 mM HEPES

buffer (pH 7.4), with decreasing urea concentrations starting at 6 M and transitioning in a stepwise

fashion from 6 M for 2 h, 4 M overnight, 2 M for 2 h, down to 0 M, repeating the 0 M step 3 times

at 1 h each, all at 4°C. Protein concentrations were calculated by BCA assay (Thermoscientific;

Waltham, MA) according to manufacturer's instructions. All subunits were stored at 4°C for

further use.

Western blot visualization

All samples were first resolved using a 15% Tris-glycine SDS-PAGE gel. After electrophoresis,

the stacking portion of the gel was removed and the resolving portion was equilibrated in transfer

buffer, allowing time for SDS to diffuse out, thus enhancing protein transfer. The PDVF membrane

was first activated by submersion in 100% methanol for 10 seconds and then equilibrated in Toubin

transfer buffer (Bio-Rad; Hercules, CA) for 15 min. Samples were transferred onto the PVDF

membrane using Bio-Rad Turbo-blot Transfer Machine using the Bio-Rad defined settings specific

for mini gel transfers of standard molecular weight proteins. The membrane was removed and

washed 3 times for 15 min with Tris-buffered saline containing 0.1% Tween-20 (TBS-T). The

membrane was then blocked with 4% milk in TBS-T for 30 min and washed with TBS-T. The

rabbit sera containing the subunit-specific antibodies (New England peptide; Gardner, MA) were

diluted 1:10,000 in TBS-T containing 4% milk and applied to the membrane overnight, rocking at

4°C. The membrane was washed with TBS-T, and an HRP-conjugated IgG goat anti-rabbit

secondary antibody (Jackson Immunoresearch; West Grove, PA) diluted 1:20,000 in TBS-T containing 4% milk was applied to the membrane for 30 min with rocking at room temperature. The membrane was washed and visualized by chemiluminescence using ECL solution adapted from [45].

Size exclusion chromatography

1 mg each of CdtB and CdtC were combined for 24 h in 5 mL of 20 mM Tris (pH 7.4) containing 150 mM NaCl, gently rocking at 4°C. This was then concentrated to <500 µL using a Vivaspin™ concentrator (GE Healthcare; Chicago, IL) with a 1 kDa MWCO. The concentrated sample was separated by size exclusion chromatography (SEC) using Sephadex® G-75 resin (GE Healthcare) at a flow rate of 1 mL/min, measuring the absorbance at 280 nm. Key fractions were combined and concentrated after identification by SDS-PAGE and Coomassie stain.

ATP agarose pull-down assay

100 µL of ATP-conjugated agarose beads (Sigma; St. Louis, MO) was added to a 1.7 mL microcentrifuge tube. Beads were pelleted at 2,000 × g for 3 min and washed twice with 1 mL PBS to remove any preservatives and broken beads. The remaining beads were blocked with 1 mL of PBS containing 0.1% bovine serum albumin for 30 min at 37°C and then washed twice with PBS. 250 ng of a toxin subunit was added to the beads in 1 mL total volume for a 30 min, 37°C incubation. The beads were pelleted at 2,000 × g for 3 min, the supernatant was collected, and the beads were washed twice with PBS. 100 µL of sample buffer was added to the beads, which were then boiled for 10 min. The collected supernatant was lyophilized before resuspension in 100 µL of sample buffer and boiled. 20 µL of the bead sample and 5 µL of the supernatant sample was

resolved via SDS-PAGE and visualized by Western blot. Unconjugated or GTP-conjugated agarose beads (Sigma) were used in an identical manner. For the competition assays, 250 ng of CdtB was pre-treated with 10 mM ATP or GTP for 30 min at 37°C. An identical procedure was used for pull-downs with 250 ng of a CdtB/CdtC heterodimer that was previously after isolated by SEC.

ATPase assay

HrpA and the individual Cdt subunits were used in a modified regenerative ATPase assay, adapted from [46, 47]. A 20x master mix (20 mM NADH, 150 mM phosphoenolpyruvate, and ~10 U/mL of pyruvate kinase/lactate dehydrogenase mixture (Sigma)) was combined in 25 mM HEPES-Tris with 100 mM K^+-glutamate, 12 mM magnesium acetate, 0.05% octyl glucose neopentyl glycol, and 14 mM β-mercaptoethanol (pH 7.6). 2x assay mixes were prepared in assay buffer supplemented with 200 µM ATP or 200 µM GTP. 30 µL of the assay mix and 30 µL of protein (final concentration at 100 nM for HrpA or 500 nM for each individual Cdt subunits) were combined; 50 µL was then transferred into a 96-well plate. The oxidation of NADH was recorded every minute over 90 min, measuring the absorbance at 340 nm. After subtracting the measurement of a reaction mixture absent of protein, a slope was generated by taking the linear regression of accumulated measurements and converted to µM of ATP turnover per mol of enzyme per min using Prism 8 (GraphPad; San Diego, CA). Blank subtraction and unit conversion was carried out using Microsoft Excel (Microsoft; Redmond, Wa).

Cellular viability assay

Wildtype and TZM cells lacking protein disulfide isomerase (PDI) were cultured in Dulbecco's Modified Eagle Medium (DMEM) supplemented with 5% fetal bovine serum and antibiotic-antimycotic until reaching 80% confluency in a 10 cm dish [48]. Cells were lifted using 1 mL of Gibco™ (ThermoScientific) Trypsin-EDTA and diluted 1:20 into a 96-well plate until reaching 80% confluency overnight. Cells were washed twice and then incubated with various combinations of Cdt subunits overnight at 37°C in serum-free media. Before addition to the cells, the Cdt subunit combinations were assembled overnight at 4°C with each subunit at concentration of 1 µg/mL. Cells were then washed twice to remove unbound toxin and incubated in toxin-free, serum-containing media for another 48 h. As a control for cell death, a set of unintoxicated cells were incubated with 10% DMSO in DMEM for 20 min. All cells were washed twice before viability was determined using an MTS assay according to the manufacturer's protocol (Promega; Madison, WI).

Circular Dichroism (CD)

CdtB at 1 mg/mL was dialyzed three times against 1 L of 20 mM phosphate buffer (pH 7.4) for 2 h per exchange. Spectral measurements using 150 µg of dialyzed CdtB in 200 µL volume with a 1 mm pathlength quartz cuvette were averaged after 5 scans, using the accumulation feature of the JASCO (Tokyo, Japan) spectral analysis software. As a reference, a blank spectral measurement was generated with filter-sterilized phosphate buffer (pH 7.4). The spectrum of the blank was then subtracted from the spectrum of CdtB alone or CdtB with 500 µM ATP. All spectral scans were taken using a JASCO J-1100 Circular Dichroism Spectropolarimeter between the 260-200 nm

region at a scanning speed of 10 nm/min with a data pitch of 0.1 nm and a digital integration time (D.I.T.) of 4 sec.

CHAPTER 4: RESULTS

Isolation of the CdtB/CdtC complex using functionally pure subunits

After initial purification of the available Cdt subunits, there was an unexpected increase in individual subunit kDa size for each subunit compared to the size of the native subunits without signal sequences. DNA sequencing revealed there was a 24 amino acid linker present between the N-terminal hexahistidine tag and protein sequence for each subunit. This was subsequently removed by 'Round-the-horn site-directed mutagenesis. After sequences of the re-cloned Cdt subunits were verified correct and absent of mutation, the individual recombinant subunits were re-purified. The average yield of purified CdtA, CdtB and CdtC per 1 L of bacterial culture was 4.5, 6, and 6.4 mg, respectively. A representative SDS-PAGE gel of the purified subunits is shown in Fig. 5A. Polyclonal antibodies were previously generated against the individual subunits containing the N-terminal extension using a for-fee service (New England Peptide; Gardner, MA). Those antibodies are specific for their cognate subunit, without cross-reactivity to the other two native subunits (Fig. 5B).

Functionality of the refolded subunits was verified by MTS assay and SEC. Assembly into a functional holotoxin with the individual subunits was observed *in vivo* by measuring cellular viability using an MTS assay. Various combinations of Cdt subunits were incubated with wildtype and PDI-deficient TZM cells. Consistent with the known toxicity of CDT, only exposure to CDT holotoxin resulted in a decrease in cellular viability (Fig. 6) [49]. This demonstrated that each of the recombinant subunits was refolded correctly and could spontaneously assemble into a

functional holotoxin. This also shows that PDI is not required for disassembly for a cytotoxic effect compared to other AB toxins that contain disulfide linkages [32].

After confirming CdtA, CdtB, and CdtC spontaneously assembled into a functional holotoxin, the CdtB/CdtC heterodimer was then isolated. CdtB and CdtC were combined overnight, followed by SEC using Sephadex® G-75 resin to separate the CdtB/CdtC heterodimer from the unassembled CdtB and CdtC subunits. There were two peaks present in the SEC absorbance (Fig. 7A). Samples from the collected fractions were resolved by SDS-PAGE and visualized by Coomassie stain (Fig. 7B). Fractions 20-23 were collected due to equal band intensities for CdtB and CdtC that represent the heterodimer eluting off the column. Fractions 11-19 that make up the first peak were not collected due to dimers of CdtB and dimers of CdtC present when visualized by Western blot (data not shown).
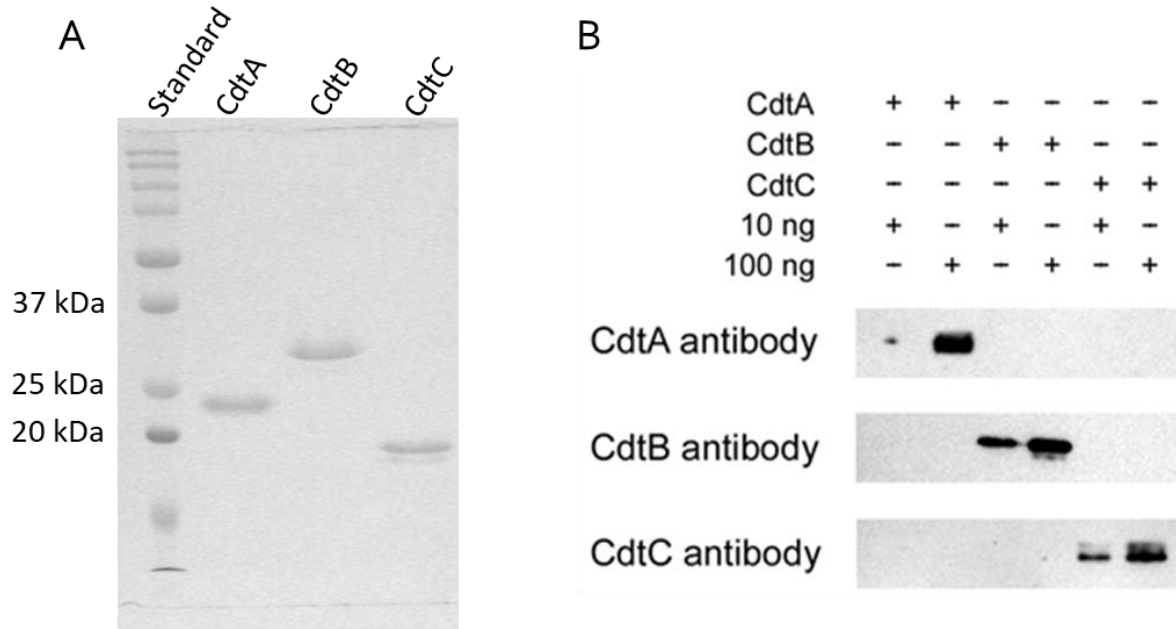
Figure 5: Purification of individual Cdt subunits and antibody specificity.

(A) CdtA, CdtB and CdtC were purified by affinity chromatography using TALON cobalt resin.

After protein refolding, 2 µg of each subunit was resolved using a 15% Tris-glycine SDS-PAGE

gel and visualized by Coomassie stain. (B) The individual subunits at the indicated amounts were

resolved by 15% Tris-glycine SDS-PAGE gel and detected by Western blot with anti-CdtA, anti-

CdtB, or anti-CdtC polyclonal antibodies.
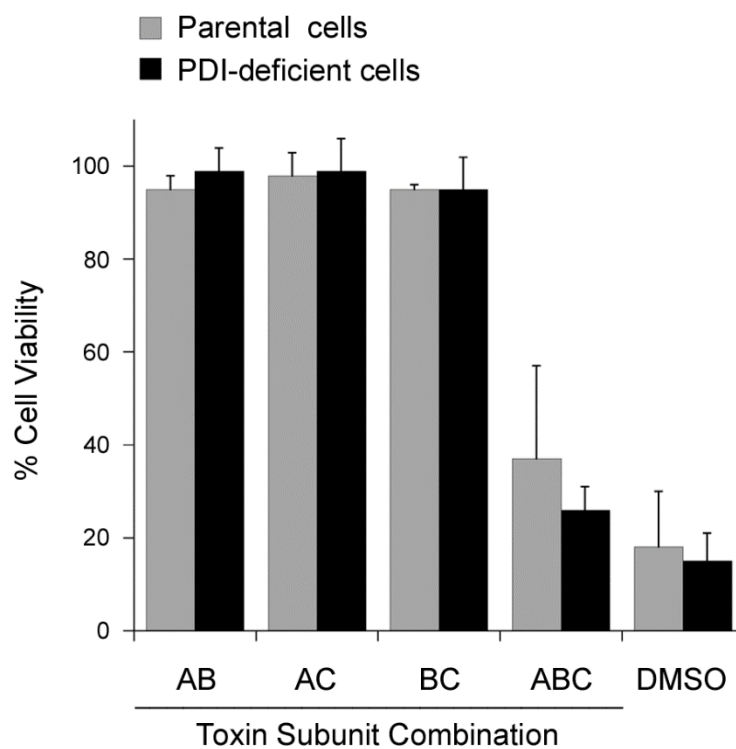
Figure 6: Cellular viability measured by MTS after CDT intoxication.
Wildtype and PDI-deficient TZM cells were incubated overnight with various combinations of Cdt subunits that were allowed to first assemble overnight. Cellular viability was measured by MTS assay after 72 h from the initial toxin exposure. For a positive control, both cell types were also incubated with 10% DMSO for 20 min.
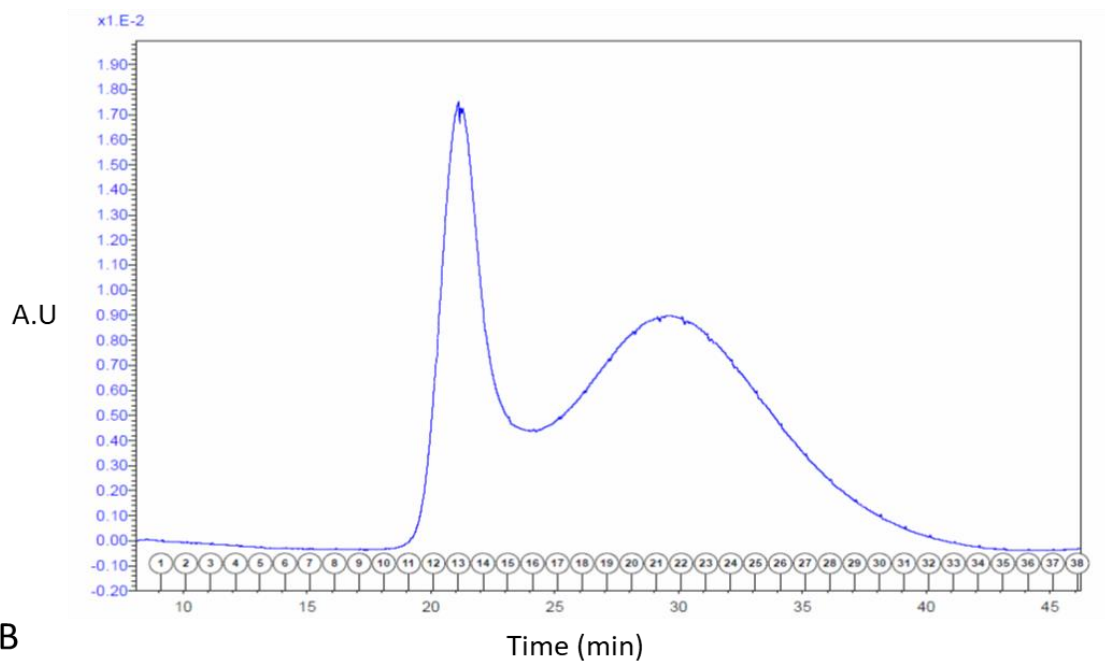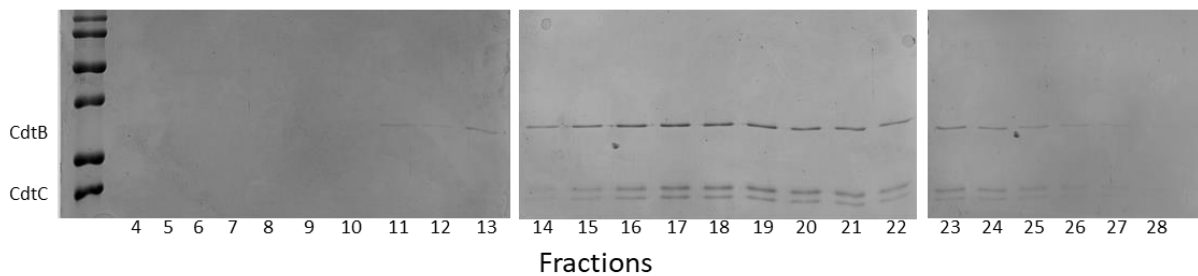
Figure 7: Isolation of CdtB/CdtC heterodimer by SEC.

(A) 1 mg each of CdtB and CdtC were combined, incubated overnight at 4 °C, and separated using Sephadex G-75 resin at a flow rate of 1 mL/min. Protein elutions were measured by absorbance at 280 nm (A. U.). (B) Fractions 4-28 were collected and visualized by 15% Tris-glycine SDS-PAGE gel and Coomassie stain. Fractions are labeled to their corresponding lane.

CdtB binds to ATP but is not an ATPase

After functionality was demonstrated, we investigated if CdtA, CdtB, or CdtC can bind to ATP. 250 ng of CdtA, CdtB, or CdtC were incubated individually with ATP-conjugated or GTP-conjugated agarose beads for 30 min at 37°C. The beads were washed to remove unbound subunits, resuspended in sample buffer, boiled, and then visualized by Western blot. Only CdtB was detectable in the pellet after incubation (Fig. 8A). These results demonstrated that CdtB is the only subunit that binds to ATP. CdtB bound to GTP as well, whereas CdtA and CdtC did not (Fig. 8A). ATP binding was eliminated by pre-treating CdtB with 10 mM of soluble ATP for 30 min before the addition to the beads (Fig. 8B). Furthermore, CdtB was not detected in association with unconjugated agarose beads. This verifies that CdtB was binding to ATP.

Since CdtB can bind to ATP, we determined whether this subunit functions as an ATPase. Using a regenerative GTPase assay modified for ATPase activity, 100 µM ATP along with either 500 nM of CdtA, CdtB, or CdtC were combined and indirectly measured for ATP hydrolysis. After subtracting the natural decay of ATP, a rate of µM of ATP being regenerated (ADP being converted back to ATP), per mol of subunit in solution, per min was calculated from the average of 3 reactions. No subunit exhibited ATPase function (Fig. 9), indicating that ATP hydrolysis does not induce disassembly. This also shows that CdtA and CdtC were not released from the ATP-agarose beads due to ATP hydrolysis, which strengthened our interpretation of the ATP pulldown assay. The RNA helicase, HrpA, was used a positive control. A similar assay determined that none of the Cdt subunits exhibited GTPase activity.
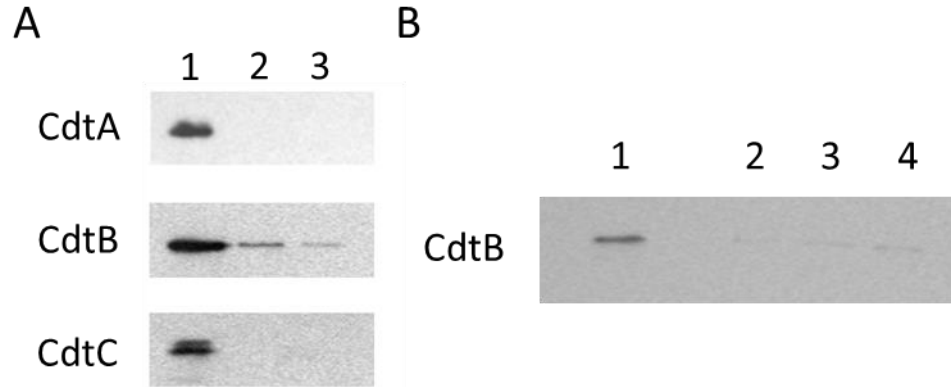
Figure 8: Only CdtB is able to bind ATP and GTP.

(A) 250 ng of CdtA, CdtB, or CdtC were incubated with ATP-conjugated (lane 2) or GTP-conjugated (lane 3) agarose beads for 30 min. The beads were then pelleted, washed, and resuspended in 100 µL of sample buffer. 20 ng of pure individual subunit (lane 1) was used as a loading control for the Western blot. (B) 250 ng of CdtB was incubated with ATP-conjugated agarose beads (lane 1) or unconjugated agarose beads (lane 2) for 30 min. 250 ng of CdtB was pretreated with 10 mM of soluble ATP (lane 3) or 10 mM soluble GTP (lane 4) for 30 minutes, then incubated with ATP-conjugated agarose beads for 30 min and visualized in the same manner as (A).
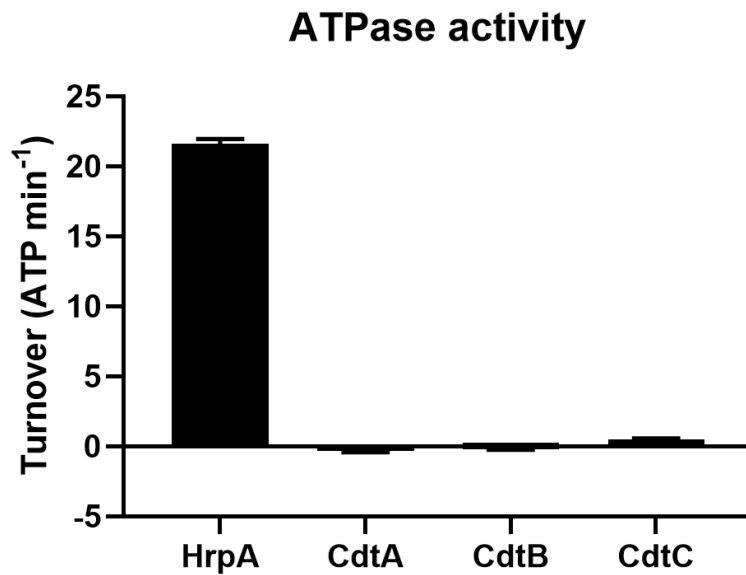
ATPase activity

Figure 9: No Cdt subunit functions as an ATPase.

100 nM HrpA, 500 nM of CdtA, CdtB, or CdtC were measured for ATPase activity using a regenerative assay containing 100 µM ATP. The graph represents the combined average of 3 reactions with standard deviation included.

ATP induced the disassembly of CdtB/CdtC but did not alter CdtB's overall structure

After identifying that only CdtB is binding to ATP, we wanted to verify that CdtC was not blocking the ATP binding site in the CdtB/CdtC heterodimer. 250 ng of the CdtB/CdtC heterodimer was incubated for 30 min at 37 °C with ATP-conjugated agarose beads. Both the supernatant and the beads were probed by Western blot. CdtB was detected in both the pellet and supernatant samples. Surprisingly, CdtC was only detected in the supernatant (Fig. 10A), indicating (i) CdtC does not block the ATP-binding site in CdtB and (ii) CdtC dissociated from CdtB bound to ATP-conjugated agarose beads. The use of GTP-conjugated agarose beads generated similar results as ATP-conjugated agarose beads (Fig. 10B). Thus, binding of either ATP or GTP to CdtB will cause the release of CdtC.

To better understand ATP's role in the CdtB/CdtC disassembly mechanism, we investigated if ATP causes a structural change that is inducing dissociation. Using CD, far-UV spectral scans of CdtB's overall secondary structure were generated with and without ATP. There is one minima present around 210 nm with both conditions. This distinct spectral characteristic is associated with a protein's secondary structure having a higher percentage of beta sheet structure than alpha helical structure. This is true for CdtB as verified by the holotoxin crystal structure [7]. After the addition of ATP, no major changes are distinguished when comparing the two CdtB spectra, indicating that ATP does not change the overall secondary structure of CdtB (Fig. 11). This suggests that the disassembly of CdtB/CdtC may be caused by a mechanism other than a structure change in CdtB.
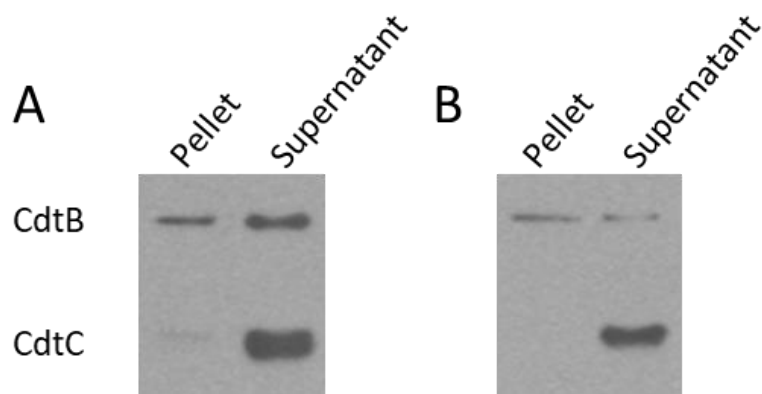
Figure 10: ATP-induced disassembly of the CdtB/CdtC heterodimer by ATP-conjugated agarose beads.

250 ng of the CdtB/CdtC heterodimer isolated by SEC was incubated with ATP-conjugated agarose beads for 30 min. The supernatant was collected and lyophilized, while the beads (pellet) were washed, and then both were resuspended sample buffer. All samples were resolved by 15% Tris-glycine SDS-PAGE gel and visualized by Western blot.
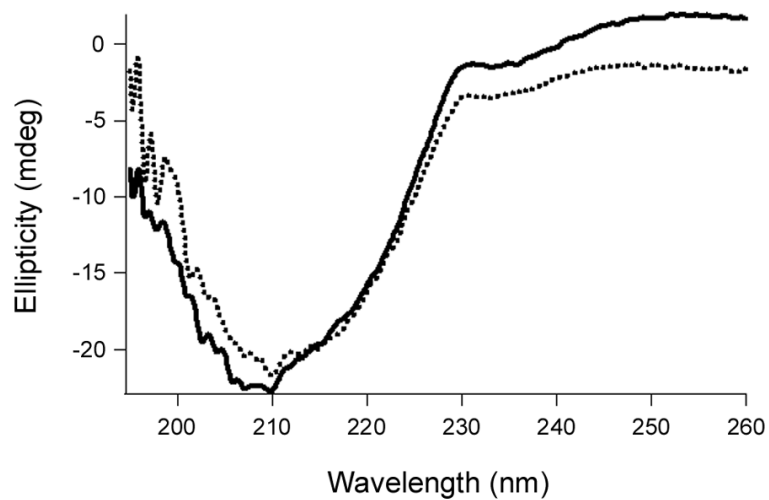
Figure 11: ATP does not alter the overall secondary structure of CdtB.

The far-UV spectra of CdtB at 100 µg/mL with 500 µM ATP (dotted line) or without ATP (solid

line) in 20 mM phosphate buffer (pH 7.4) are presented. One of the experiments is shown, with

each spectrum representing the average of five scans after buffer subtraction.

CHAPTER 5: DISCUSSION

Here we have presented evidence that ATP plays a critical role in the novel two-stage disassembly of CDT. Although the CDT holotoxin binds to the cell surface, CdtA dissociates before reaching the Golgi apparatus [21]. This is the first stage of disassembly. The loss of CdtC, presumably in the ER, represents the second stage of disassembly [10]. CdtC dissociation for CdtB activity is required since the DNase I active site is blocked by the N-terminal tail of CdtC [7, 11, 29].

Currently, there are many studies on CDT including the identification of the surface receptor, the intracellular trafficking route, and the cellular response mechanisms to the DNA damage caused by CDT [6, 19, 21]. There are currently no studies that detail the molecular basis for disassembly of CDT. Previously, it has been shown that PT disassembles in the ER after ATP binds to the PTB pentamer [34-36]. Preliminary results generated from the Teter lab indicated that the addition of ATP will also cause the disassembly of the CdtB/CdtC heterodimer. After purification of the functional individual Cdt subunits and isolation of the CdtB/CdtC heterodimer, we demonstrated that ATP induces CdtB/CdtC disassembly by binding to CdtB. However, ATP binding did not cause an overall change to the secondary structure of CdtB. Furthermore, CdtB did not hydrolyze ATP. The use of the GTP generated similar results, demonstrating that this mechanism is not specific to only ATP. This likely represents a nucleotide-binding site present in CdtB, and further testing using CTP and TTP is needed to confirm this.

It is currently understood that assembly of the CDT holotoxin is 100% efficient [50, 51]. Since there are no monomers detected from the SEC profile, this would serve as a confirmation and could

be validated by performing SEC after assembling the CdtB/CdtC heterodimer with one subunit at an excess. The use of native-PAGE electrophoresis would confirm that the CdtB/CdtC heterodimer is isolated, validating the ATP- and GTP-conjugated agarose results. This method could serve as an alternative to modeling disassembly as well.

Future studies using crystallography with CdtB and ATP are needed to (i) identify the location of CdtB's ATP-binding pocket, and (ii) any subtle structural changes not detectable by CD. The location of the ATP-binding pocket could potentially be in the groove between CdtB and CdtC. In this scenario, ATP would be functioning as a competitive inhibitor for CdtB that acts as a wedge separating the two subunits. Alternatively, ATP's interaction with CdtB could perhaps be functioning as an allosteric regulator altering the intrachain interactions in CdtB as ATP binds, inducing CdtC dissociation. Additional experimentation with the CDT holotoxin will address if CdtA has an inhibitory effect on the ATP-induced disassembly CdtB/CdtC heterodimer. This could be caused by CdtA blocking the ATP-binding pocket, or as an alternative, CdtA could be stabilizing the protein-protein interaction between CdtA and CdtC. A mutagenesis study that introduces point mutations into the active site of the ATP-binding pocket will further identify the amino acids that are required to induce the disassembly of the CdtB/CdtC heterodimer.

The CD method of measuring changes to secondary structure of CdtB is not without limitation due to ATP absorbing light in the far UV region [52]. Attempts to increase the ATP concentration higher than what were described here produced spectra with unacceptable signal to noise ratios. However, the concentration of ATP might not be high enough to induce a conformational change to be seen by conventional biophysical approaches. Furthermore, the lack of an overall structural

change in CdtB with ATP using CD does not rule out possible changes to local structure at the tested concentration of 200 µM ATP. While the predominant beta sheet structure remained unchanged, there may be unfolding and refolding of partial alpha helical structures. These changes could possibly be distinguished by a change in protease sensitivity that was previously used to demonstrate CdtB's thermal stability [53]. This would be confirmed by crystallography with CdtB and ATP.

We have shown here that CDT is the second AB toxin that appears to use an ATP-induced disassembly mechanism as a part of its overall two-stage disassembly process. This mechanism may act as a molecular sensor upon ATP binding to CdtB that causes the disassembly of the CdtB/CdtC heterodimer that is triggered by the initial interaction of ATP after toxin delivery to the ER.

LIST OF REFERENCES

1.   Fais, T., et al., *Impact of CDT Toxin on Human Diseases.* Toxins (Basel), 2016. **8**(7).

2.   Steen, R., *Eradicating chancroid.* Bull World Health Organ, 2001. **79**(9): p. 818-26.

3.   Marks, M., et al., *Challenges and key research questions for yaws eradication.* Lancet Infect Dis, 2015. **15**(10): p. 1220-1225.

4.   Gonzalez-Beiras, C., et al., *Epidemiology of Haemophilus ducreyi Infections.* Emerg Infect Dis, 2016. **22**(1): p. 1-8.

5.   Wising, C., et al., *Induction of apoptosis/necrosis in various human cell lineages by Haemophilus ducreyi cytolethal distending toxin.* Toxicon, 2005. **45**(6): p. 767-76.

6.   Jinadasa, R.N., et al., *Cytolethal distending toxin: a conserved bacterial genotoxin that blocks cell cycle progression, leading to apoptosis of a broad range of mammalian cell lineages.* Microbiology, 2011. **157**(Pt 7): p. 1851-75.

7.   Nesic, D., Y. Hsu, and C.E. Stebbins, *Assembly and function of a bacterial genotoxin.* Nature, 2004. **429**(6990): p. 429-33.

8.   Berman, H.M., et al., *The Protein Data Bank and the challenge of structural genomics.* Nat Struct Biol, 2000. **7 Suppl**: p. 957-9.

9.   Boesze-Battaglia, K., et al., *Cytolethal distending toxin-induced cell cycle arrest of lymphocytes is dependent upon recognition and binding to cholesterol.* J Biol Chem, 2009. **284**(16): p. 10650-8.

10.   Guerra, L., et al., *Cellular internalization of cytolethal distending toxin: a new end to a known pathway.* Cell Microbiol, 2005. **7**(7): p. 921-34.

11.   Nesic, D. and C.E. Stebbins, *Mechanisms of assembly and cellular interactions for the bacterial genotoxin CDT.* PLoS Pathog, 2005. **1**(3): p. e28.

12.   Eshraghi, A., et al., *Cytolethal distending toxin family members are differentially affected by alterations in host glycans and membrane cholesterol.* J Biol Chem, 2010. **285**(24): p. 18199-207.

13.   Fahrer, J., et al., *Cytolethal distending toxin (CDT) is a radiomimetic agent and induces persistent levels of DNA double-strand breaks in human fibroblasts.* DNA Repair (Amst), 2014. **18**: p. 31-43.

14.   Frisan, T., et al., *The Haemophilus ducreyi cytolethal distending toxin induces DNA double-strand breaks and promotes ATM-dependent activation of RhoA.* Cell Microbiol, 2003. **5**(10): p. 695-707.

15.   Li, L., et al., *The Haemophilus ducreyi cytolethal distending toxin activates sensors of DNA damage and repair complexes in proliferating and non-proliferating cells.* Cell Microbiol, 2002. **4**(2): p. 87-99.

16.   Svensson, L.A., P. Henning, and T. Lagergard, *The cytolethal distending toxin of Haemophilus ducreyi inhibits endothelial cell proliferation.* Infect Immun, 2002. **70**(5): p. 2665-9.

17.   Boesze-Battaglia, K., et al., *A journey of cytolethal distending toxins through cell membranes.* Front Cell Infect Microbiol, 2016. **6**(81).

18.   Hontz, J.S., et al., *Differences in crystal and solution structures of the cytolethal distending toxin B subunit: Relevance to nuclear translocation and functional activation.* J Biol Chem, 2006. **281**(35): p. 25365-72.

19.   Gargi, A., et al., *Cellular interactions of the cytolethal distending toxins from Escherichia coli and Haemophilus ducreyi.* J Biol Chem, 2013. **288**(11): p. 7492-505.

20.   Frisan, T., *Bacterial genotoxins: The long journey to the nucleus of mammalian cells.* Biochim Biophys Acta, 2016. **1858**(3): p. 567-75.

21.   Cortes-Bratti, X., et al., *Cellular internalization of cytolethal distending toxin from Haemophilus ducreyi.* Infect Immun, 2000. **68**(12): p. 6903-11.

22.   Dixon, S.D., et al., *Distinct Roles for CdtA and CdtC during Intoxication by Cytolethal Distending Toxins.* PLoS One, 2015. **10**(11): p. e0143977.

23.   Deng, K. and E.J. Hansen, *A CdtA-CdtC complex can block killing of HeLa cells by Haemophilus ducreyi cytolethal distending toxin.* Infect Immun, 2003. **71**(11): p. 6633-40.

24.   Damek-Poprawa, M., et al., *Localization of Aggregatibacter actinomycetemcomitans Cytolethal Distending Toxin Subunits during Intoxication of Live Cells.* Infect Immun, 2012. **80**(8): p. 2761-70.

25.   Frisan, T., *20 - Bacterial genotoxins*, in *The Comprehensive Sourcebook of Bacterial Protein Toxins (Fourth Edition)*, J. Alouf, D. Ladant, and M.R. Popoff, Editors. 2015, Academic Press: Boston. p. 558-602.

26.   Baeuerle, P.A. and W.B. Huttner, *Tyrosine sulfation is a trans-Golgi-specific protein modification.* J Cell Biol, 1987. **105**(6 Pt 1): p. 2655-64.

27.   Breitling, J. and M. Aebi, *N-linked protein glycosylation in the endoplasmic reticulum.* Cold Spring Harb Perspect Biol, 2013. **5**(8): p. a013359.

28.   Guerra, L., et al., *The biology of the cytolethal distending toxins.* Toxins (Basel), 2011. **3**(3): p. 172-90.

29.   Hu, X., D. Nesic, and C.E. Stebbins, *Comparative structure-function analysis of cytolethal distending toxins.* Proteins, 2006. **62**(2): p. 421-34.

30.   Sixma, T.K., et al., *Crystal structure of a cholera toxin-related heat-labile enterotoxin from E. coli.* Nature, 1991. **351**(6325): p. 371-7.

31.   Zhang, R.G., et al., *The three-dimensional crystal structure of cholera toxin.* J Mol Biol, 1995. **251**(4): p. 563-73.

32.   Taylor, M., et al., *Protein-disulfide isomerase displaces the cholera toxin A1 subunit from the holotoxin without unfolding the A1 subunit.* J Biol Chem, 2011. **286**(25): p. 22090-100.

33.   Stein, P.E., et al., *The crystal structure of pertussis toxin.* Structure, 1994. **2**(1): p. 45-57.

34.   Plaut, R.D., et al., *Intracellular disassembly and activity of pertussis toxin require interaction with ATP.* Pathog Dis, 2016. **74**(6).

35.   Hazes, B., et al., *Crystal structure of the pertussis toxin-ATP complex: a molecular sensor.* J Mol Biol, 1996. **258**(4): p. 661-71.

36.   Hausman, S.Z., C.R. Manclark, and D.L. Burns, *Binding of ATP by pertussis toxin and isolated toxin subunits.* Biochemistry, 1990. **29**(26): p. 6128-31.

37.   Clairmont, C.A., A. De Maio, and C.B. Hirschberg, *Translocation of ATP into the lumen of rough endoplasmic reticulum-derived vesicles and its binding to luminal proteins including BiP (GRP 78) and GRP 94.* J Biol Chem, 1992. **267**(6): p. 3983-90.

38.   Maxfield, F.R. and D.J. Yamashiro, *Endosome acidification and the pathways of receptor-mediated endocytosis.* Adv Exp Med Biol, 1987. **225**: p. 189-98.

39.   Medaglia, M.V. and R.J. Fisher, *Analysis of Interacting Proteins with Surface Plasmon Resonance Using Biacore*, in *Protein-Protein Interactions*, E. Golemis, Editor. 2002, Cold Spring Harbor Laboratory Press: Cold Spring Harbor, New York. p. 255-272.

40.   Homola, J., *Present and future of surface plasmon resonance biosensors.* Anal Bioanal Chem, 2003. **377**(3): p. 528-39.

41.   Svensson, L.A., et al., *The impact of Haemophilus ducreyi cytolethal distending toxin on cells involved in immune response.* Microb Pathog, 2001. **30**(3): p. 157-66.

42.   Xu, T., et al., *Interactions of Haemophilus ducreyi and purified cytolethal distending toxin with human monocyte-derived dendritic cells, macrophages and CD4+ T cells.* Microbes Infect, 2004. **6**(13): p. 1171-81.

43.   Bertani, G., *Lysogeny at mid-twentieth century: P1, P2, and other experimental systems.* J Bacteriol, 2004. **186**(3): p. 595-600.

44.   OpenWetWare. *'Round-the-horn site-directed mutagenesis.* 10 December 2018 22:18 UTC [cited 2019 June 2]; Available from: https://openwetware.org/mediawiki/index.php?title=%27Round-the-horn_site-directed_mutagenesis&oldid=1055958.

45.   Chung, C.T., S.L. Niemela, and R.H. Miller, *One-step preparation of competent Escherichia coli: transformation and storage of bacterial cells in the same solution.* Proc Natl Acad Sci U S A, 1989. **86**(7): p. 2172-5.

46.   Ingerman, E. and J. Nunnari, *A continuous, regenerative coupled GTPase assay for dynamin-related proteins.* Methods Enzymol, 2005. **404**: p. 611-9.

47.   Wingo, R.J., et al., *Exacerbation of [delta]efp sickness in Escherichia coli by an uncharacterized RNA helicase.* p. 1 online resource (xiv, 82 pages).

48.   Ou, W. and J. Silver, *Role of protein disulfide isomerase and other thiol-reactive proteins in HIV-1 envelope protein-mediated fusion.* Virology, 2006. **350**(2): p. 406-17.

49.   Lara-Tejero, M. and J.E. Galan, *CdtA, CdtB, and CdtC form a tripartite complex that is required for cytolethal distending toxin activity.* Infect Immun, 2001. **69**(7): p. 4358-65.

50.   Cao, L., et al., *Characterization of point mutations in the cdtA gene of the cytolethal distending toxin of Actinobacillus actinomycetemcomitans.* Mol Microbiol, 2005. **58**(5): p. 1303-21.

51.   Cao, L., et al., *Role of aromatic amino acids in receptor binding activity and subunit assembly of the cytolethal distending toxin of Aggregatibacter actinomycetemcomitans.* Infect Immun, 2008. **76**(7): p. 2812-21.

52.   Ito, A. and T. Ito, *Absorption spectra of deoxyribose, ribosephosphate, ATP and DNA by direct transmission measurements in the vacuum-UV (150-190 nm) and far-UV (190-260 nm) regions using synchrotron radiation as a light source.* Photochem Photobiol, 1986. **44**(3): p. 355-8.

53.   Guerra, L., et al., *A novel mode of translocation for cytolethal distending toxin.* Biochim Biophys Acta, 2009. **1793**(3): p. 489-95.